Available online at www.sciencedirect.com
SCIENCE DIRECT®
Journal of Power Sources 119–121 (2003) 125–129
JOURNAL OF POWER SOURCES
www.elsevier.com/locate/jpowsour

Crystal structure and cathode performance dependence on oxygen content of $LiMn_{1.5}Ni_{0.5}O_4$ as a cathode material for secondary lithium batteries

Yasushi Idemoto*, Hirosuke Narai, Nobuyuki Koura

Department of Pure and Applied Chemistry, Faculty of Science and Technology, Tokyo University of Science, 2641 Yamazaki, Noda, Chiba 278-8510, Japan

Abstract

$LiMn_{1.5}Ni_{0.5}O_4$, as a 5 V cathode material, was prepared by changing synthesis method and heat treatment. We investigated the dependence of its properties, crystal structure and cathode performance on the oxygen content. The oxygen content of the samples (sol–gel method and annealed at a high P_{O_2}) increased in comparison with the sample prepared by the solid-state method. The charge–discharge curves of the samples (solid-state method) had plateaus at 4.1 and 4.7–5.0 V. The 4.1 V plateau disappeared for the samples made by the sol–gel method or annealed at a high P_{O_2}. The discharge capacity with respect to cycle number of the 5 V region in the $LiMn_{1.5}Ni_{0.5}O_4$ (sol–gel method) electrodes shows an especially good cycle performance. The neutron-diffraction intensity profiles of $LiMn_{1.5}Ni_{0.5}O_4$ were analyzed. From these results, the samples are assigned to the ordered form (space group $P4_332$). The amount of the impurity phase decreases by annealing at a high P_{O_2} or using the sol–gel method. Furthermore, the distortion of the Mn, Ni(12d)-O octahedral site was restrained by increasing oxygen content.

Keywords: Lithium manganese spinel; Crystal structure; Oxygen content; Cathode material; Neutron diffraction; Nickel substitution

1. Introduction

The lithium manganese oxide spinel, as a positive electrode material for rechargeable lithium batteries, has a 4.7–4.9 V plateau when 3d-transition metals are substituted for Mn to make $LiMn_{2-x}M_xO_4$ (M = Co, Cr, Cu, Fe, Ni) [1,2]. $LiMn_{1.5}Ni_{0.5}O_4$ especially has a good electrode performance. However, this material prepared by the solid-state method, has a 4.1 V plateau which is related to the Mn oxidation of +3 to +4. Dahn et al. reported that $LiMn_{1-x}Ni_xO_4$ loses oxygen and disproportionates into a spinel with a smaller Ni content, in samples heated above ca. 650 °C [1]. Recently, it has been reported that the 4.1 V plateau of $LiMn_{2-x}Ni_xO_4$ was eliminated when using the sol–gel method [1], the composite carbonate process [3], and self-reaction method [4].

In this study, we intended to investigate the change in the crystal structure and cathode performance dependence on the oxygen content for $LiMn_{1.5}Ni_{0.5}O_4$ by changing the heat treatment and synthesis method. The oxidation state of the 3d-transition metal and oxygen content was determined by iodometry and the ICP method. The crystal structure was determined by Rietveld analysis using powder neutron diffraction data.

2. Experimental

$LiMn_{1.5}Ni_{0.5}O_4$ powders were prepared by reacting a stoichiometric mixture of $^7Li_2CO_3$, MnO_2 and $Ni(OH)_2$. The mixture was preheated at 600 °C for 24 h in air, then heated at 700 °C for 24 h in O_2 (solid-state method). Furthermore, the powder obtained by the solid-state method was annealed at 500 °C for 24 h in P_{O_2} = 2.02 MPa. A sample was prepared by the sol–gel method using $LiNO_3$, $Mn(NO_3)_2{\cdot}9H_2O$, and $Ni(NO_3)_2{\cdot}6H_2O$ precursors and PVA with subsequent decomposition at 150 °C. The resulting solids were heated at 500 °C for 24 h in O_2, then calcined at 700 °C for 24 h in O_2. These samples were examined by powder X-ray diffraction and the metal composition was determined by ICP. The Mn valence was determined by chemical analysis [5].

The crystal structure of $LiMn_{1.5}Ni_{0.5}O_4$ was studied by neutron powder diffraction using the HERMES [6] of IMR at the JPR-3M reactor in JAERI. The data were refined with the Rietveld technique using the Rietan 2000 program [7].

* Corresponding author. Tel.: +81-4-7124-1501; fax: +81-4-7125-7761.
E-mail address: idemoto@rs.noda.tus.ac.jp (Y. Idemoto).

0378-7753/03/$ – see front matter © 2003 Elsevier Science B.V. All rights reserved.
doi:10.1016/S0378-7753(03)00140-X

The oxygen nonstoichiometry was measured using a microbalance, the sensitivity of which is 1 μg, and the weight change was determined as a function of the temperature and oxygen partial pressure. The particle sizes of the samples were observed by SEM. The surface areas of the samples were determined by the BET method.

A three-electrode electrochemical cell consisting of a $LiMn_{1.5}Ni_{0.5}O_4$ cathode (WE) and a Li film (CE and RE) was used for testing. The cathodes were prepared by mixing a blend of the active material, acetylene black and PVDF (5:2:1) with NMP and coated onto Al foil. The electrodes was dried at 150 °C in a vacuum atmosphere, and pressed at 400 kg cm^{-2}. The electrolyte was a 1 M $LiPF_6$ in EC/DEC (1:1) solution. All procedures were carried out in a dry box with an Ar atmosphere. Cyclic voltammograms (CV) were performed from 3.5 to 5.0 V versus Li/Li^+ at a scan rate of 0.2 mV s^{-1}. Charge–discharge tests were performed at a constant current density (0.2 mA cm^{-2}) at 25 °C, with cutoff potentials of 3.5–5.0 V versus Li/Li^+.

3. Results and discussion

3.1. Sample characterization

The X-ray diffraction patterns of the $LiMn_{1.5}Ni_{0.5}O_4$ prepared by the solid-state method showed two phases, which are mainly a cubic spinel and a small amount of impurities ($Li_yNi_{1-y}O$). On the other hand, the sample that was prepared by the sol–gel method, had a single cubic phase. The lattice parameter, a, of is sample, which was annealed at a high P_{O_2} or prepared by the sol–gel method, is decreased in comparison with that of the sample prepared by the solid-state method [8].

The metal composition of these samples was determined by ICP. The resulting metal composition was almost same as the nominal composition. The Mn valence was determined by chemical analysis, which assumed that the Ni valence was 2.0. The oxygen content was evaluated from the metal composition and Mn valence using electroneutral conditions. The Mn valence, oxygen content and lattice parameter, which was determined by XRD, are shown in Table 1. The Mn valence and oxygen content of the sample, which was annealed at a high P_{O_2} or prepared by the sol–gel method, increased in comparison with those of the sample which was prepared by the solid-state method. The Mn valence of the sample (sol–gel method) is almost 4. The lattice parameter, a, decreases with the increasing oxygen content.

Table 1
Mn valence, oxygen content and lattice constant of $LiMn_{1.5}Ni_{0.5}O_4$

$LiMn_{1.5}Ni_{0.5}O_4$	Mn valence	Oxygen content	Lattice constant (nm)
Solid-state method	3.874(3)	3.899(3)	0.81751(2)
500 °C, 60 h, P_{O_2} = 2.02 MPa annealed	3.997(7)	3.990(7)	0.81720(2)
Sol–gel method	3.934(7)	3.927(7)	0.81731(6)

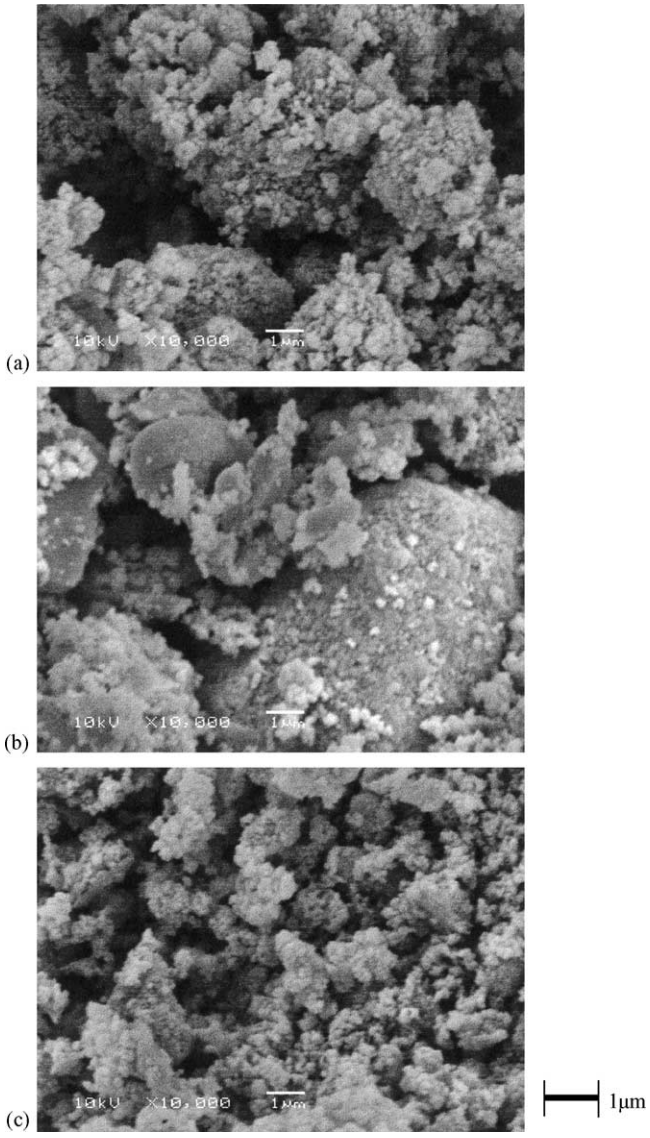

Fig. 1. SEM photographs of $LiMn_{1.5}Ni_{0.5}O_4$. (a) Solid-state method, (b) 500 °C, 60 h, P_{O_2} = 2.02 MPa annealed, (c) sol–gel method.

Fig. 1 shows the SEM images of the sample morphology. The particle size of the sample, prepared by the sol–gel method, is small and homogeneous. The surface area of the sample, prepared by the sol–gel method, is large in comparison with that of the sample prepared by the solid-state method.

3.2. Oxygen nonstoichiometry

The oxygen nonstoichiometry was measured by thermogravimetric analysis. The weight change caused by the abrupt change in the oxygen partial pressure was followed with time, and the equilibrium weight and the oxygen content were determined. From these results, it was shown that $LiMn_{1-x}Ni_xO_4$ has a large nonstoichiometry above

Table 2
Final results of Rietveld refinement for $LiMn_{1.5}Ni_{0.5}O_4$, which prepared by solid-state method, using HERMES in space group $P4_332$ (cubic, $Z = 8$)

Atom	Site	x	y	z	$100 \times B$ (nm^2)	Site occupancy
Ni1	4b	0.625	0.625	0.625	0.27(16)	0.69(1)
Mn1	4b	$=x$(Ni1)	$=y$(Ni1)	$=z$(Ni1)	$=B$(Ni1)	0.31(1)
Li	8c	1.004(1)	1.004(1)	1.004(1)	0.71(22)	1
Mn2	12d	0.125	0.374(1)	−0.124(1)	1	0.9167
Ni2	12d	$=x$(Mn2)	$=y$(Mn2)	$=z$(Mn2)	$=B$(Mn2)	0.0833
O1	8c	0.3861(3)	0.3861(3)	0.3861(3)	0.74(13)	1
O2	24e	0.1022(4)	0.1256(4)	0.3928(3)	0.54(8)	0.89(1)

Numbers in parentheses were estimated standard deviations of the last significant digit, and those without deviations were fixed. $R_{wp} = 7.75\%$, $R_p = 6.06\%$, $R_{exp} = 5.02\%$, $S = 1.54$, $a = 0.8166(1)$ nm. $LiMn_{1.5}Ni_{0.5}O_4$:$Li_yNi_{1-y}O$ ($a = 0.41484(2)$ nm) = 09813:0.0187.

600 °C. This suggested that oxygen deficiency occurred when samples were prepared above 600 °C.

3.3. Structural analysis by neutron diffraction data

The neutron-diffraction intensity profiles of $LiMn_{1.5}Ni_{0.5}O_4$ were analyzed over a wide range. The samples were prepared by mixing $^7Li_2CO_3$ with MnO_2 and $Ni(OH)_2$ so as to avoid the high neutron absorption of ^6Li. From these results, it was shown that the sample prepared by the sol–gel method is single phase. However, the samples prepared by the solid-state method or annealed at a high P_{O_2} included a small amount of the $Li_yNi_{1-y}O$ impurity phase. The amount of the impurity phase decreased by annealing at a high P_{O_2}.

The crystal structure of ordered spinels (space group $P4_332$) for $LiFe_5O_8$ was refined from the neutron analysis by Marin et al. [9]. The crystal structure of $LiNi_{0.5}Mn_{1.5}O_4$ has been studied by neutron diffraction [10] and the cation order characterized by the space group $P4_332$. However, a detailed crystal structure determination was not achieved.

An initial refinement was carried out by assuming 16*d* Wyckoff positions for the disordered cubic spinel (space group: *Fd*-3*m*) or 4*b* + 12*d* for the ordered one (space group $P4_332$). Based on these results, many reflections cannot be indexed according to the space group *Fd*-3*m*, on the other hand, they can be assigned to the space group $P4_332$. We then compared the goodness-fit indicator, $S = R_{wp}/R_e$. The S value, which is 1.54, of the ordered form ($P4_332$) is significantly lower than that of 4.97 for the disordered form (*Fd*-3*m*). Accordingly, the data were analyzed assuming the ordered form ($P4_332$) and the samples, which were prepared by the solid-state method or annealed at a high P_{O_2}, were refined from the two phase model including $Li_yNi_{1-y}O$. The final refined parameters for $LiMn_{1.5}Ni_{0.5}O_4$, which was prepared by the solid-state method, in space group $P4_332$ (cubic, $Z = 8$) are shown in Table 2. Fig. 2 illustrates the results of the Rietveld refinement patterns for samples prepared by (a) the solid-state method, and (b) annealed at a high P_{O_2}. Good agreement between the observed and calculated patterns was obtained with a low R-factor. The lattice parameter of the second phase of $Li_yNi_{1-y}O$ is 0.41484(2) nm, almost the same as that of $Li_yNi_{1-y}O$ ($y = 0.18$) [1]. The oxygen content and Ni content of the cubic phase ($LiMn_{1.5}Ni_{0.5}O_4$) for the samples, which were prepared by the sol–gel method and annealed at a high P_{O_2}, increase in comparison to those of the samples prepared by solid-state method, and the tendency is similar to the above chemical analysis results.

Fig. 3 shows the relation between the bond lengths of Mn2, Ni2(12d)-O and the oxygen content for $LiMn_{1.5}Ni_{0.5}O_4$. The bond length of Mn2, Ni2-O2* increases and that of Mn2, Ni2-O1 decreases with increasing oxygen content. Hence, the distortion of the Mn, Ni(12d)-O octahedral site is restrained with increasing oxygen content.

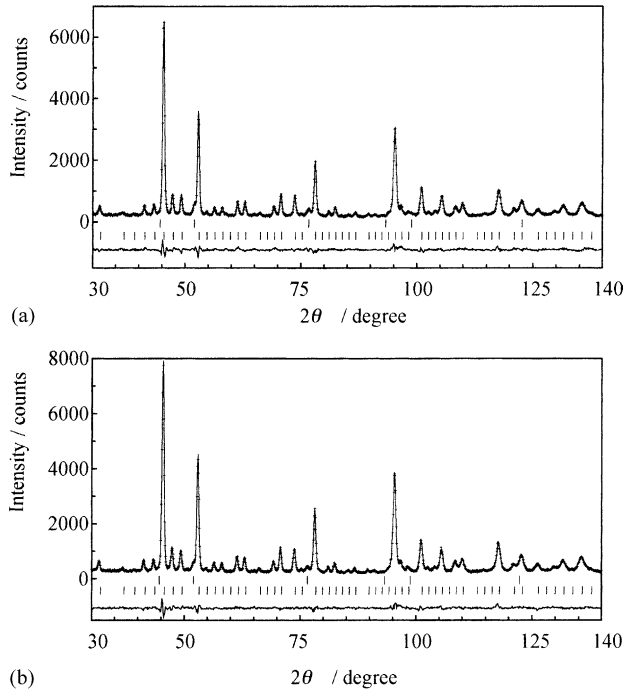

Fig. 2. Rietveld refinement patterns for $LiMn_{1.5}Ni_{0.5}O_4$. Plus marks show observed neutron diffraction intensities and a solid line represents calculated intensities. The vertical marks below patterns indicate the positions of allowed Bragg reflections (upper: $Li_yNi_{1-y}O$, bottom: cubic, $Z = 8$, space group, $P4_332$). The curve at the bottom is the difference between the observed and calculated intensities in the same scale. (a) Solid-state method, (b) 500 °C, 60 h, $P_{O_2} = 2.02$ MPa annealed.

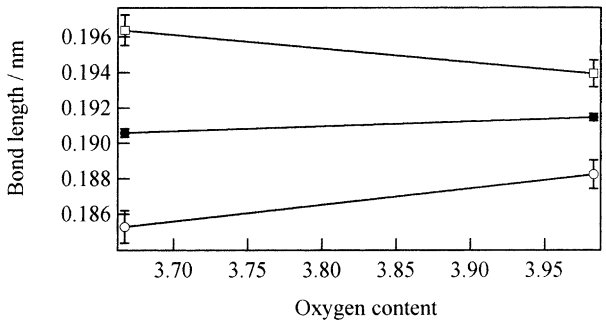

Fig. 3. Relation between bond length of Mn2, Ni2(12d)-O and oxygen content for $LiMn_{1.5}Ni_{0.5}O_4$. (○) Mn2, Ni2-O2*; (●) Mn2, Ni2-O2**; (□) Mn2, Ni2-O1. O2*: $z-$ 1/2, 1/2 − x, $-y$; O2**: y, z, x.

3.4. Electrode characteristics

Fig. 4 shows the galvanostatic charge–discharge curves of the $LiMn_{1.5}Ni_{0.5}O_4$ samples. The charge–discharge curves of the samples synthesized by the solid-state method appear as plateaus at 4.1 and 4.7–5.0 V. On the other hand, the 4.1 V plateau disappeared for sample synthesized by annealing with a high P_{O_2} treatment or by the sol–gel method. These results are consistent with the CV data. The discharge capacity as a function of cycle number of Li|$LiMn_{1.5}Ni_{0.5}O_4$ cells at room temperature is shown in Table 3. The discharge capacity with respect to cycle number in the 5 V region for $LiMn_{1.5}Ni_{0.5}O_4$, which was synthesized by the sol–gel method, retains its initial capacity after 100 cycles.

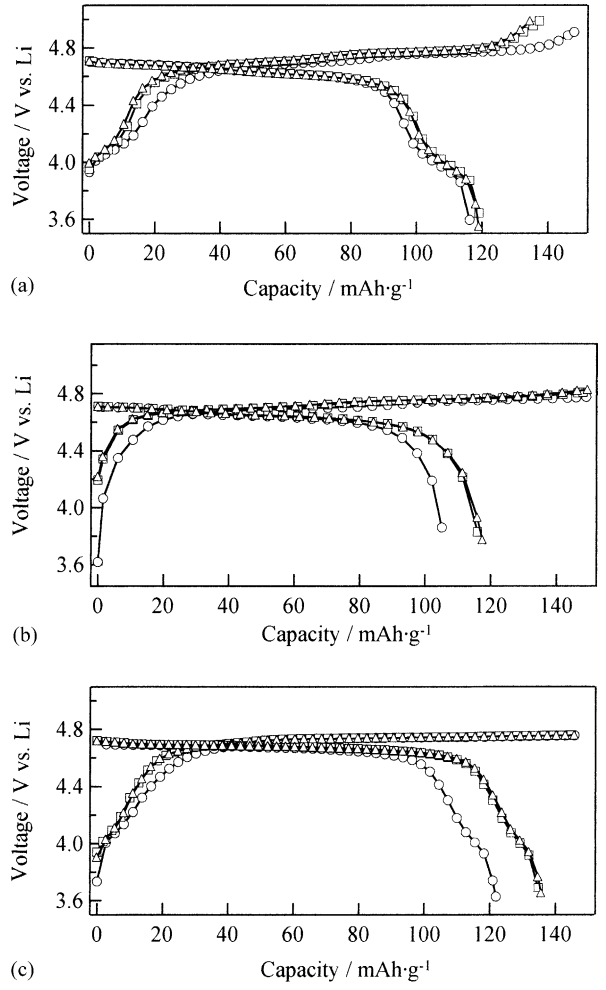

Fig. 4. Galvanostatic charge–discharge curves of $LiMn_{1.5}Ni_{0.5}O_4$ at 25 °C and 0.2 mA cm^{-2}. (a) Solid-state method, (b) 500 °C, 60 h, P_{O_2} = 2.02 MPa annealed, (c) sol–gel method. (○) 1st cycle, (□) 2nd cycle, (△) 3rd cycle.

Table 3
Discharge capacity change (discharge capacity relative to maximum of discharge capacity (%)) of Li|$LiMn_{1.5}Ni_{0.5}O_4$ cell at room temperature and 0.2 mA cm^{-2}

Cycle number	10	20	40	60	80	100
Solid-state method	97.7	96.0	94.7	92.3	89.5	84.9
High P_{O_2} annealing	98.7	94.6	88.4	81.8	75.8	71.7
Sol–gel method	100.0	100.0	100.0	100.0	100.0	99.8

Cutoff voltage: 3.6–5.0 V vs. Li.

4. Conclusions

$LiMn_{1.5}Ni_{0.5}O_4$ as a 5 V cathode materials were prepared by changing the synthesis method and heat treatment. The oxygen content and Mn valence of the samples (once made by sol–gel method and once annealed at a high P_{O_2}) increased in comparison with the sample prepared by the solid-state method. From the structural analysis results based on the neutron-diffraction intensity profiles of $LiMn_{1.5}Ni_{0.5}O_4$, these samples are assigned to the ordered form (cubic, space group: $P4_332$). The amount of the impurity phase decreases and the oxygen content and Ni content of the cubic phase ($LiMn_{1.5}Ni_{0.5}O_4$) increases by annealing at a high P_{O_2} or preparation by the sol–gel method. Furthermore, the distortion of the Mn, Ni(12d)-O octahedral site was restrained by the increased oxygen content.

The charge–discharge curves of the samples (solid-state method) had plateaus at 4.1 and 4.7–5.0 V. The 4.1 V plateau disappeared for samples made by the sol–gel method or annealed at a high P_{O_2}. This is related to the increase in the Mn valence and oxygen content. The discharge capacity with respect to cycle number of the 5 V region in the $LiMn_{1.5}Ni_{0.5}O_4$ (sol–gel method) electrodes shows an especially good cycle performance. This is related to the homogeneity, small particle size, and the large surface area of the sample, and should be related to the structural changes.

Acknowledgements

We were indebted to Dr. A. Toubou, Dr. K. Ooyama, and Prof. Y. Yamaguchi (Tohoku University) for measurement of the powder neutron diffraction at HERMES (JPR-3M).

References

[1] Q. Zhong, A. Banakdarpour, M. Zhang, Y. Gao, J.R. Dahn, J. Electrochem. Soc. 144 (1997) 205.
[2] T. Ohzuku, S. Takeda, M. Iwanaga, J. Power Sources 81–82 (1999) 90.
[3] S. Ota, K. Kobayashi, K. Yamato, K. Hayashi, H. Kitamura, T. Miyashita, in: Proceedings of the Meeting Abstracts of the 41st Battery Symposium, Nagoya, Japan, 2000, p. 452.
[4] A. Mori, T. Endo, H. Hashiba, K. Takahashi, in: Proceedings of the Meeting Abstracts of the 41st Battery Symposium, Nagoya, Japan, 2000, p. 456.
[5] Y. Idemoto, K. Udagawa, N. Koura, Electrochemistry 67 (1999) 235.
[6] K. Ohoyama, T. Kanouchi, K. Nemoto, M. Ohashi, T. Kajitani, Y. Yamaguchi, Jpn. J. Appl. Phys. 37 (1998) 3319.
[7] F. Izumi, T. Ikeda, Mater. Sci. Forum 321–324 (2000) 198.
[8] Y. Idemoto, H. Narai, N. Koura, Electrochemistry 70 (2002) 587.
[9] S.J. Marin, M. O'Keeffe, D.E. Partin, J. Solid State Chem. 113 (1994) 413.
[10] D. Gryffroy, R.E. Vandenberghe, E. Legrand, Mater. Sci. Forum 79–82 (1991) 785.